

# Kinetic network model to explain gain-of-function mutations in ERK2 enzyme

Cite as: J. Chem. Phys. **150**, 155101 (2019); <https://doi.org/10.1063/1.5088647>

Submitted: 12 January 2019 • Accepted: 24 March 2019 • Published Online: 16 April 2019

Mikita Misiura and  Anatoly B. Kolomeisky



View Online



Export Citation



CrossMark

## ARTICLES YOU MAY BE INTERESTED IN

[Target search on DNA by interacting molecules: First-passage approach](#)

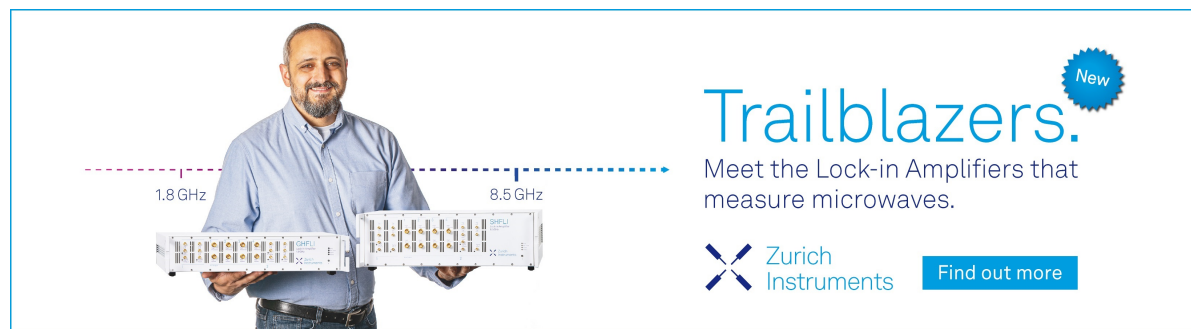
The Journal of Chemical Physics **151**, 125101 (2019); <https://doi.org/10.1063/1.5123988>


[The effect of obstacles in multi-site protein target search with DNA looping](#)

The Journal of Chemical Physics **152**, 025101 (2020); <https://doi.org/10.1063/1.5135917>


[Variational selection of features for molecular kinetics](#)

The Journal of Chemical Physics **150**, 194108 (2019); <https://doi.org/10.1063/1.5083040>



**Trailblazers.** 

Meet the Lock-in Amplifiers that measure microwaves.

 Zurich Instruments [Find out more](#)

# Kinetic network model to explain gain-of-function mutations in ERK2 enzyme

Cite as: J. Chem. Phys. 150, 155101 (2019); doi: 10.1063/1.5088647

Submitted: 12 January 2019 • Accepted: 24 March 2019 •

Published Online: 16 April 2019



View Online



Export Citation



CrossMark

Mikita Misiura<sup>1,2</sup> and Anatoly B. Kolomeisky<sup>1,2,3,a)</sup> 

## AFFILIATIONS

<sup>1</sup>Department of Chemistry, Rice University, Houston, Texas 77005-1892, USA

<sup>2</sup>Center for Theoretical Biological Physics, Rice University, Houston, Texas 77005-1892, USA

<sup>3</sup>Department of Chemical and Biomolecular Engineering, Rice University, Houston, Texas 77005-1892, USA

<sup>a)</sup>Electronic mail: [tolya@rice.edu](mailto:tolya@rice.edu)

## ABSTRACT

ERK2 is a kinase protein that belongs to a Ras/Raf/MEK/ERK signaling pathway, which is activated in response to a range of extracellular signals. Malfunctioning of this cascade leads to a variety of serious diseases, including cancers. This is often caused by mutations in proteins belonging to the cascade, frequently leading to abnormally high activity of the cascade even in the absence of an external signal. One such “gain-of-function” mutation in the ERK2 protein, called a “sevenmaker” mutation (D319N), was discovered in 1994 in *Drosophila*. The mutation leads to disruption of interactions of other proteins with the D-site of ERK2 and results, contrary to expectations, in an increase of its activity *in vivo*. However, no molecular mechanism to explain this effect has been presented so far. The difficulty is that this mutation should equally negatively affect interactions of ERK2 with all substrates, activators, and deactivators. In this paper, we present a semiquantitative kinetic network model that gives a possible explanation of the increased activity of mutant ERK2 species. A simplified biochemical network for ERK2, viewed as a system of coupled Michaelis-Menten processes, is presented. Its dynamic properties are calculated explicitly using the method of first-passage processes. The effect of mutation is associated with changes in the strength of interaction energy between the enzyme and the substrates. It is found that the dependence of kinetic properties of the protein on the interaction energy is nonmonotonic, suggesting that some mutations might lead to more efficient catalytic properties, despite weakening intermolecular interactions. Our theoretical predictions agree with experimental observations for the sevenmaker mutation in ERK2. It is also argued that the effect of mutations might depend on the concentrations of substrates.

Published under license by AIP Publishing. <https://doi.org/10.1063/1.5088647>

## I. INTRODUCTION

Mitogen-activated protein (MAP) kinase ERK2 (Extracellular Signal-Regulated Kinase 2) is an enzyme that plays an important role in a variety of biochemical processes. It is activated in response to several extracellular signals such as mitogens, interleukins, growth factors, and cytokines,<sup>1,2</sup> operating as a part of the Ras/Raf/MEK/ERK signaling pathway, which is crucial for cell functioning.<sup>3–5</sup> ERK2 is a small 42 kDa protein, consisting of C-terminal and N-terminal domains.<sup>6–8</sup> It is an ATP-dependent enzyme and its ATP-binding site, as well as the catalytic site, is located in the region between the main domains. Unlike many enzymes, ERK2 does not bind its substrates in the immediate vicinity of the catalytic site, but instead it utilizes the so-called recruiting (docking) sites, which are located 15–20 Å away from the place where the

catalysis occurs. These binding sites are usually referred to as the D-recruiting site (DRS) and the F-recruiting site (FRS), and they are responsible for recognition of multiple substrates with different structures.<sup>9–19</sup>

To become catalytically active, ERK2 requires phosphorylation of two of its residues: Tyr185 and Thr183.<sup>20</sup> Phosphorylation leads to alteration of mutual orientation of domains and their dynamics.<sup>7,21–25</sup> Activation of ERK2 is normally done by MAP/ERK kinases (MEK).<sup>26</sup> Active ERK2, in its turn, can be deactivated by a number of phosphatases.<sup>1,20</sup> Combination of these two processes—activation and deactivation—enables precise control of ERK2 activity, providing a robust and efficient method to respond to external signals. Since ERK2 regulates many critically important processes, including cell growth, cell differentiation, and cell proliferation, the alteration of its normal enzymatic activity can lead to serious negative effects,

such as uncontrollable tissue growth, which was shown to be linked to a variety of diseases, including cancers.<sup>27–30</sup>

An interesting example of ERK2 malfunctioning is the existence of gain-of-function mutations inside the Ras/Raf/MEK/ERK signaling pathway. Such mutations can alter the structure of one of the kinases in a phosphorylation cascade, thus preventing the activity of ERK2 from being regulated properly and eventually leading to diseases.<sup>3,30</sup> The most known gain-of-function mutation in ERK2 (D319N) is called “sevenmaker,” which was discovered in *Drosophila* in 1994 as a result of genetic screenings for mutations that activate the sev signaling pathway in the absence of signals.<sup>31–34</sup> The mutation is located in the DRS (docking site) of ERK2 in the common domain (CD) region.<sup>35</sup>

The fact that the sevenmaker mutation activates the enzyme is rather surprising because it is expected that this mutation should negatively influence interactions of ERK2 with all substrates, activators, and deactivators in a similar fashion. One would then suggest that the mutation should lower the enzymatic activity. Indeed, there are experimental observations<sup>35,36</sup> suggesting that many substrates, activators (including MEK), and deactivators use the DRS site and, in particular, the CD domain to recognize the ERK2 protein. They interact using a so-called kinase interaction motif (KIM), which consists of 2–3 positively charged Lys and/or Arg residues.<sup>19</sup> Thus, the sevenmaker mutation should disrupt all ERK2-involving processes in the similar way, and so it is surprising that it can lead to an apparent increase of ERK2 activity *in vivo*.<sup>31,32</sup> Despite the fundamental importance of ERK2, molecular mechanisms of its gain-of-function mutations (and specifically, the sevenmaker mutation) remain not well understood. One proposal to explain these observations is based on the fact that there are only two ERK2 activators, MEK1 and MEK2, while there are many deactivators. It was suggested that some deactivators might be less affected by the disrupted interaction with the CD domain.<sup>35</sup> To support this, there are experimental data showing that the mutation D319N in the ERK2 is less sensitive to dephosphorylation.<sup>32,37</sup> However, that does not resolve the problem entirely since the ability of ERK2 to phosphorylate substrates should be also reduced by a comparable amount because the same molecular interactions are involved in both catalytic processes.<sup>35</sup>

In this paper, we propose a theoretical model that quantitatively explains the effect of the sevenmaker mutation. It is based on the kinetic network description of the system with the additional assumption that the mutation equally modifies interaction energies between ERK2 and all substrates, activators, and deactivators.

By analyzing a simplified regulation network of ERK2, built as a system of several coupled Michaelis-Menten processes, the kinetic properties of ERK2 proteins are evaluated explicitly via the first-passage method. It is shown that the effective chemical kinetic properties in these systems might change nonmonotonically as a function of the interactions. This suggests that some mutations might lead to more efficient catalytic properties of ERK2 protein variants, despite the decrease of the interaction energies. It is argued that this is a possible molecular mechanism of gain-of-function mutations in ERK2, explaining the experimental observations on the sevenmaker mutation.

## II. THEORY

### A. Kinetic network model

To clarify the molecular mechanisms of increased activity for the sevenmaker mutation, one should analyze the kinetic properties of the biochemical regulation pathway of ERK2. Although it is known that ERK2 functioning involves many biochemical states and transitions, we consider a minimal simplified version of the regulation scheme as presented in Fig. 1. Our idea is to approximate the regulation network as three coupled Michaelis-Menten processes that correspond to main processes involving the enzyme: activation, inactivation, and ERK2-mediated phosphorylation.<sup>1</sup>

In the state 0 (labeled as ERK2), the enzyme molecule is inactive (not phosphorylated) and it can bind MEK enzyme with a rate constant  $u$  to reach the state 1 (labeled as ERK2·M); see Fig. 1. ERK2 requires a phosphorylation of two residues, but in this work, we model the phosphorylation as one step to simplify the calculations. This simplification does not affect the main conclusions of our work. From the state 1, ERK2 can return back to the state 0 with a rate  $w$  by dissociating from the complex with MEK, or it can be phosphorylated to reach the state 2 (ppERK2) with a rate  $\alpha$ . After that, ppERK2 can either be dephosphorylated through the formation of a complex with a phosphatase (state 3, ERK2·D) with the rate constant  $u$ , or it can remain active and phosphorylate its own substrates by forming the substrate-enzyme complex with the rate constant  $u$  (state 4, ppERK2·S), and producing the product (state 5, ppERK2+P) with the rate  $\alpha$ .

It is important to note that in this model, we consider a single ERK2 enzyme molecule, because it is not consumed during the chemical reactions, and fixed concentrations of other participants. However, the results for arbitrary concentrations of ERK2 can be easily generalized.

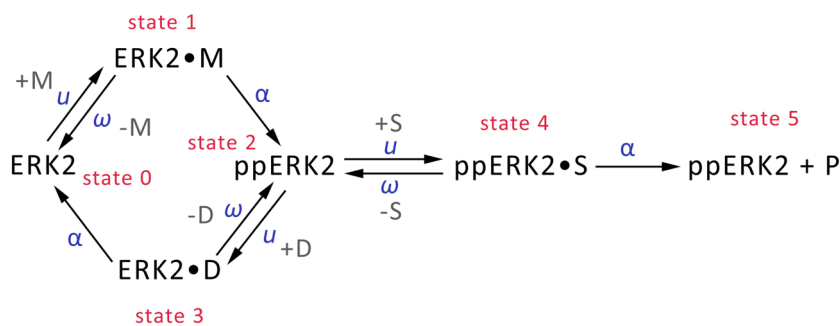


**FIG. 1.** A simplified biochemical regulation scheme for ERK2 considered in this work. First, ERK2 must be phosphorylated by MEK (denoted as M) to become an active enzyme and to phosphorylate its substrates (denoted as S). At the same time, the phosphatase (denoted as D) can dephosphorylate ERK2 to return it to the inactive state. More details are given in the text.

To simplify calculations, in this model, we assume that the corresponding rate constants in all Michaelis-Menten reactions for different processes are equal to each other so that there are only three kinetic parameters in the system:  $u$ ,  $w$ , and  $\alpha$ . This assumption is based on the fact that all enzymatic processes are taking place at the same location and they involve chemical species that have similar nature. This assumption is reasonable because all activators, deactivators, and substrates use the same binding sites on ERK2, and mutations in ERK2 will most probably cause similar (although clearly not entirely identical) changes to their binding energies. However, it is also important to notice that relaxing this condition (making all corresponding rates different) will not qualitatively change the main theoretical predictions of this work, while it will make the mathematical calculations much more complicated. As an additional confirmation of our arguments, in the [supplementary material](#), we present results from kinetic Monte Carlo simulations using variable sets of kinetic rates (Figs. S6–S9), which fully agree with the qualitative trends predicted by the simplest reduced model with identical transition rates.

To evaluate catalytic properties of the system, we employ a method of first-passage processes that was successfully utilized for analyzing multiple processes in chemistry, physics, and biology.<sup>38,39</sup> The idea is to introduce a first-passage probability density function  $F_n(t)$ , which is defined as a probability to complete the reaction (i.e., to reach the final state 5 for the first time, [Fig. 1](#)) at time  $t$  if at  $t = 0$  the system was in the state  $n$ . In another words,  $F_n(t)$  is related to a survival probability  $S_n(t)$ , which describes a probability that a molecule starting in the state  $n$  did not react up to time  $t$ . More specifically,  $F_n(t) = \partial[1 - S_n(t)]/\partial t$ . Determining these functions will provide a full dynamic description of the catalytic process in this system. The temporal evolution of first-passage probabilities is governed by a set of the backward master equations,<sup>38,39</sup> which are closely related to standard chemical kinetics equations

$$\frac{dF_0(t)}{dt} = u_M F_1(t) - u_M F_0(t), \quad (1)$$

$$\frac{dF_1(t)}{dt} = \alpha F_2(t) + w F_0(t) - (w + \alpha) F_1(t), \quad (2)$$

$$\frac{dF_2(t)}{dt} = u_D F_3(t) + u_S F_4(t) - (u_D + u_S) F_2(t), \quad (3)$$

$$\frac{dF_3(t)}{dt} = \alpha F_0(t) + w F_2(t) - (w + \alpha) F_3(t), \quad (4)$$

$$\frac{dF_4(t)}{dt} = \alpha F_5(t) + w F_2(t) - (w + \alpha) F_4(t). \quad (5)$$

Please note that these equations differ from standard forward master equations that deal with probabilities to be found at the specific sites, while in our case, we consider the probabilities to start at the specific site and to reach the final state. In these equations, we take into account the fact that the association transition rates are proportional to the concentrations of participants, i.e.,

$$u_X = uX, \quad (6)$$

where  $X = M, D$ , or  $S$ , which represent the concentration of activator, deactivator, and substrate, respectively. While in general concentrations of activator, deactivator, and substrate molecules will vary in time, in this work, we assume that enzymatic reactions that involve ERK2 are taking place faster than other processes affecting various substrates, and for this reason the corresponding concentrations are taken to be constant. In addition, the initial condition requires that  $F_5(t) = \delta(t)$ , which means that if the system starts in the state 5, the reaction is accomplished immediately.

To calculate the first-passage probabilities, we utilize Laplace transformations,  $\int_0^\infty e^{-st} F_n(t) dt \equiv \tilde{F}_n(s)$ . After such transformation, Eqs. (1)–(5) can be rewritten as simpler algebraic expressions

$$(s + u_M) \tilde{F}_0 = u_M \tilde{F}_1, \quad (7)$$

$$(s + \alpha + w) \tilde{F}_1 = \alpha \tilde{F}_2 + w \tilde{F}_0, \quad (8)$$

$$(s + u_S + u_D) \tilde{F}_2 = u_D \tilde{F}_3 + u_S \tilde{F}_4, \quad (9)$$

$$(s + \alpha + w) \tilde{F}_3 = \alpha \tilde{F}_0 + w \tilde{F}_2, \quad (10)$$

$$(s + \alpha + w) \tilde{F}_4 = \alpha \tilde{F}_5 + w \tilde{F}_2. \quad (11)$$

The initial condition leads to  $\tilde{F}_5(s) = 1$ . This system of equations can be easily solved. Specifically, if we start the process in the state 0, we obtain

$$\tilde{F}_0(s) = \frac{\alpha^2 u^2 MS}{A + B + \Gamma + \Delta}, \quad (12)$$

where parameters in the denominator are defined as

$$A = \alpha^2 [usD + (uM + s)(s + uS)], \quad (13)$$

$$B = s^2 (uM + s + w)(uD + s + uS + w), \quad (14)$$

$$\Gamma = \alpha s [2u^2 MS + 2s(s + w)], \quad (15)$$

$$\Delta = u(2s + w)(M + S) + uD(2uM + 2s + w). \quad (16)$$

The explicit expressions for the first-passage probability functions provide a direct way of describing all dynamic properties in the system. For example, the average time to reach the product state 5 starting from the state 0, which is the same as the mean time for the catalytic reaction (turnover time), is given by<sup>38,39</sup>

$$T_0 \equiv -\frac{d\tilde{F}_0}{ds}(s = 0), \quad (17)$$

from which using Eqs. (12)–(16), we get

$$T_0 = \frac{2uM(S + D) + (\alpha + w)(D + M + S)}{\alpha uMS}. \quad (18)$$

This result can be better understood if we rewrite it in the Michaelis-Menten-like form with respect to the substrate  $S$  transformation ( $T_0 = 1/k_{cat} + K_M/k_{cat} * 1/S$ ) as follows,

$$T_0 = \frac{2uM + \alpha + w}{\alpha uM} + \frac{(M + D)(\alpha + w) + 2uMD}{\alpha uM} \frac{1}{S}, \quad (19)$$

from which the overall effective Michaelis-Menten parameters for the kinetic network are determined in terms of the microscopic transition rates

$$K_M = \frac{(\alpha + w)(M + D) + 2uMD}{\alpha + w + 2uM}, \quad (20)$$

$$k_{cat} = \frac{\alpha uM}{\alpha + w + 2uM}, \quad (21)$$

and

$$\frac{k_{cat}}{K_M} = \frac{\alpha uM}{(\alpha + w)(M + D) + 2uMD}. \quad (22)$$

To quantitatively analyze the effect of mutations, we assume that mutations change the strength of the interactions in the ERK2 complexes with activators, deactivators, or substrates, respectively. We define a binding energy  $\epsilon$  as a measure of strength of such interactions. The sign is chosen so that more negative values of  $\epsilon$  correspond to stronger binding. Then, the detailed balance-like arguments allow us to estimate the relations between the rate constants and the binding energy

$$\frac{u}{w} = \frac{u_0}{w_0} e^{-\beta\epsilon}, \quad (23)$$

$$\alpha = \alpha_0 e^{\beta\epsilon}. \quad (24)$$

Here, the rates with superscript 0 correspond to transition rates for the hypothetical situations when the interactions energies are equal to zero. These equations can be understood in the following way. The stronger the binding interactions, the faster the system will go into the states with the complex formation (states 1, 3, and 4) and the slower it will leave these states. Correspondingly, weaker interactions stimulate the system to preferentially break these complexes faster than to form them.

Determining enzymatic properties of the system requires explicit expressions for rates that include the effect of the interactions. To achieve that, we can rewrite the expressions for transition rates as<sup>39</sup>

$$u = u_0 e^{-\beta\theta\epsilon}, \quad (25)$$

and

$$w = w_0 e^{\beta(1-\theta)\epsilon}, \quad (26)$$

with  $\beta = 1/k_B T$ . The parameter  $0 \leq \theta \leq 1$  specifies how the interaction energy is distributed between forward and backward transitions to form or to break the complex state.<sup>39</sup> For simplicity, in the following expressions, we omit the subscript 0 so that  $u$ ,  $w$ , and  $\alpha$  now replace  $u_0$ ,  $w_0$ , and  $\alpha_0$ , respectively. With these assumptions, our final equations for the kinetic parameters are given by

$$K_M = \frac{(\alpha e^{\beta\epsilon} + w e^{\beta(1-\theta)\epsilon})(M + D) + 2u e^{-\beta\theta\epsilon} MD}{\alpha e^{\beta\epsilon} + w e^{\beta(1-\theta)\epsilon} + 2u e^{-\beta\theta\epsilon} M}, \quad (27)$$

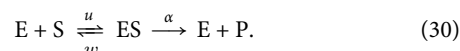
$$k_{cat} = \frac{\alpha u e^{\beta(1-\theta)\epsilon} M}{\alpha e^{\beta\epsilon} + w e^{\beta(1-\theta)\epsilon} + 2u e^{-\beta\theta\epsilon} M}, \quad (28)$$

$$\frac{k_{cat}}{K_M} = \frac{\alpha u e^{\beta(1-\theta)\epsilon} M}{(\alpha e^{\beta\epsilon} + w e^{\beta(1-\theta)\epsilon})(M + D) + 2u e^{-\beta\theta\epsilon} MD}. \quad (29)$$

The main advantage of this theoretical approach is that now the effect of mutations can be investigated quantitatively because in our language, it corresponds to varying the interaction energy  $\epsilon$ .

## B. Michaelis-Menten model

To understand better the mechanisms of the ERK2 regulation that couple together several enzymatic processes, we will be comparing them with the simplest situation that involves only a single enzymatic process. For this purpose, we present here a brief derivation of catalytic properties for a classical Michaelis-Menten kinetic scheme



The derivation follows exactly the same steps as described for the model in Fig. 1, so we only present main steps here. We assume that  $E + S$  corresponds to the state 0,  $ES$  describes the state 1, and  $E + P$  is the final state 2. The temporal evolution of the corresponding first-passage probability functions follows from

$$\frac{dF_0(t)}{dt} = u_S F_1(t) - u_S F_0(t) \quad (31)$$

and

$$\frac{dF_1(t)}{dt} = \alpha F_2(t) + w F_0(t) - (w + \alpha) F_1(t). \quad (32)$$

After the Laplace transformation, these equations can be rewritten as follows:

$$(s + u_S) \tilde{F}_0 = u_S \tilde{F}_1, \quad (33)$$

$$(s + \alpha + w) \tilde{F}_1 = \alpha \tilde{F}_2 + w \tilde{F}_0. \quad (34)$$

Solving this system of equations yields the following expression for the turnover time  $T_0$ :

$$T_0 = \frac{1}{\alpha} + \frac{w + \alpha}{u \alpha} \frac{1}{S}. \quad (35)$$

Finally, the Michaelis-Menten parameters are given by

$$K_M = \frac{\alpha + w}{u}, \quad (36)$$

$$k_{cat} = \alpha, \quad (37)$$

and

$$\frac{k_{cat}}{K_M} = \frac{\alpha u}{\alpha + w}, \quad (38)$$

where  $u$ ,  $w$ , and  $\alpha$  depend on the substrate binding energy exactly as described [see Eqs. (24)–(26)]. This derivation also explicitly shows that all chemical kinetic results for enzymatic systems can be derived using the first-passage method.

Unless stated otherwise, the following parameters are utilized for calculations in Sec. III:  $\theta = 0.5$ ,  $\alpha = w = 100 \text{ s}^{-1}$ ,  $k = 10\,000 \text{ s}^{-1} \text{ M}^{-1}$ , and  $D = M = S = 0.001 \text{ M}$ . These parameters are chosen just to illustrate our theoretical method. However, different sets of kinetic rates are explored in Monte Carlo simulations and the results are presented in the [supplementary material](#).

### C. Numerical simulations

To test the validity of our theoretical calculations, we performed extensive Kinetic Monte Carlo simulations using the Gillespie Algorithm for the chemical network that describes the system. Details of the algorithm and the results can be found in the [supplementary material](#).

## III. RESULTS AND DISCUSSION

Our main idea is that mutations of ERK2 modify the interaction energy between the enzyme and the substrate molecules, and this leads to changes in the chemical kinetic properties of the system. Using explicit expressions derived in Sec. II C, we can analyze how the enzymatic parameters for ERK2 and simple Michaelis-Menten (MM) schemes vary with the binding energy  $\epsilon$ . The results are presented in Figs. 2 and 3. One can see that the enzymatic properties of ERK2 regulation network differ significantly from the classical MM scheme. Lowering the strength of binding interactions (making  $\epsilon$  more positive) strongly increases the catalytic rate  $k_{cat}$  in the MM system, while the dependence of  $k_{cat}$  on  $\epsilon$  is nonmonotonic for the ERK2 system (see Fig. 2). It can be shown also that in this case, the highest value of  $k_{cat}$  is achieved for

$$\frac{\epsilon_{max}}{k_B T} = -\frac{\ln\left[\frac{\alpha-\theta}{2-uM}\right]}{(1+\theta)}. \quad (39)$$

Varying the interaction energy also leads to different curves for the Michaelis constant for the simple MM and for the ERK2 regulation network (Fig. 3).  $K_M$  monotonically increases with  $\epsilon$  in the MM case, while for the ERK2 system,  $K_M$  is slowly changing between two limiting behaviors. For very strong attractive interactions ( $\epsilon \rightarrow -\infty$ ), we have  $K_M \simeq D$ , while for strong repulsive interactions, ( $\epsilon \rightarrow +\infty$ )  $K_M \simeq D + M$ .

To better quantify enzymatic efficiency of ERK2 protein, it is more useful to consider a ratio  $k_{cat}/K_M$ , which is known as a specificity constant. The larger this parameter, the more efficient is the enzymatic process. Figure 4 presents specificity constants as

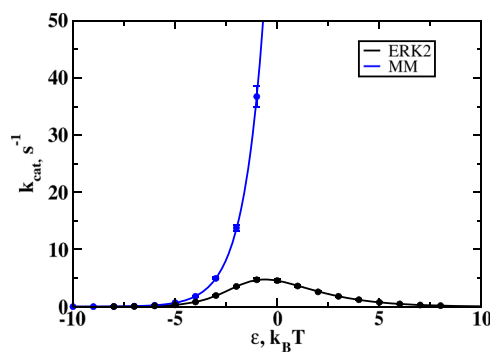


**FIG. 2.** Catalytic constants as functions of the binding energies for Michaelis-Menten (MM, blue) and ERK2 schemes. Lines are theoretical predictions, and symbols correspond to kinetic Monte Carlo simulations. Error bars show standard deviations. Negative energies correspond to stronger binding. For the MM scheme, a monotonic behavior is observed: the stronger the interaction, the lower  $k_{cat}$ ; while for the ERK2 scheme, the dependence is nonmonotonic: there is an optimal value of binding energy that produces the highest  $k_{cat}$ .

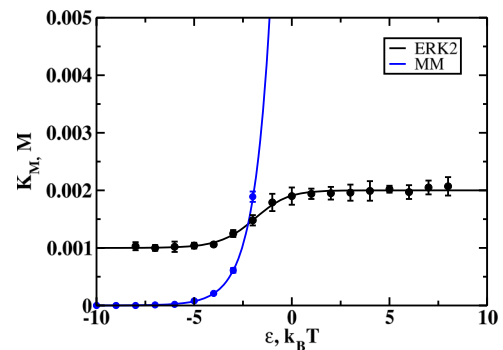


**FIG. 3.** Michaelis constants as functions of the binding energies for the Michaelis-Menten (MM) scheme (blue) and the ERK2 scheme (black). Lines are theoretical predictions, and symbols correspond to kinetic Monte Carlo simulations. Error bars show standard deviations. Negative energies correspond to stronger binding. For the MM scheme, the dependence is monotonic, and the stronger the binding, the lower the Michaelis constant. For the ERK2 scheme, the dependence is also monotonic, but  $K_M$  changes between two limits.

functions of the binding energies for both schemes, and again the classical MM behavior is strikingly different from the predictions for the ERK2 regulation system. The specificity constant for the MM process decreases monotonically with the interaction energy, while the nonmonotonic dependence is observed for the ERK2 case. The position of the maximum here is

$$\frac{\epsilon_{max}}{k_B T} = -\frac{\ln\left[\frac{(D+M)\alpha-\theta}{2\cdot k\cdot D\cdot M}\right]}{(1+\theta)}. \quad (40)$$

This result has a very important consequence for explaining the appearance of gain-of-function mutations in the ERK2 system. If one assumes that the binding energy in the WT enzyme ( $\epsilon_{WT}$ ) is negative and it does not correspond to  $\epsilon_{max}$  ( $\epsilon_{WT} < \epsilon_{max}$ ), then mutations that change the interaction energies to the range between  $\epsilon_{WT}$  and  $\epsilon_{max}$  will increase the activity of enzyme: the region between two vertical lines in Fig. 4. In this situation, the mutation that weakens the interactions with the substrate will effectively make the ERK2

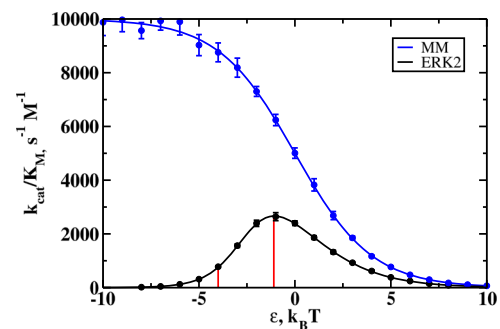


**FIG. 4.** Specificity constants ( $k_{cat}/K_M$ ) as functions of the binding energy for the Michaelis-Menten scheme (MM, blue) and for the ERK2 scheme (ERK2, black). Lines are theoretical predictions, and symbols correspond to kinetic Monte Carlo simulations. Error bars show standard deviations. Negative energies correspond to stronger binding. In the region between two vertical lines for the ERK2 scheme, the decrease of strength of interactions will lead to higher values of specificity.

regulation network more efficient in comparison with the wild type case. This might be a possible molecular mechanism of how the sevenmaker mutation operates in the ERK2 system. It is also important to note that since ERK2 is a regulatory enzyme, it is likely to operate *in vivo* at low concentrations in the regime where the specificity constant is the main property that determines the catalytic efficacy.

The effect of gain-of-function mutations can be also explained using the fluxes along the different branches of the regulation scheme presented in Fig. 1. The overall chemical process of making the product molecules with the help of ERK2 enzymes can be viewed as a molecular current along the enzymatic network. The flux that starts in the state 0 reaches the state 2 via the activation branch ( $J_a$ ), where it divides into the flux that goes to the final product via the phosphorylation branch ( $J_p$ ) and the flux that returns back to the state 0 via the deactivation branch ( $J_d$ ). In the stationary state, the flux balance requires that

$$J_a = J_d + J_p. \quad (41)$$

The overall enzymatic activity can be correlated with the product formation flux  $J_p$ . The higher is the molecular current to reach the final product, the larger is the enzymatic activity of the system. Then our theoretical picture suggests that the sevenmaker mutation lowers both  $J_a$  and  $J_d$  fluxes, but it decreases the deactivation flux more so that the product formation flux  $J_p$  in the case of mutation is larger in comparison with the WT ERK2 molecule, i.e.,  $J_p(\text{mutant}) > J_p(\text{WT})$ . The results presented in Fig. 5, where the effect of varying the deactivation flux is investigated, support these arguments. Lowering the concentration of deactivator ( $D$ ) decreases the possibility for the system to go into the deactivation branch. For low  $D$ , the enzymatic properties of the ERK2 regulation pathway, as expected, approach the simple MM scheme, and the nonmonotonic behavior as well as the ability to increase the enzyme's activity by mutation disappear. Only when there are significant fluxes via the deactivation path, the gain-of-function mutations might appear in such systems. Thus, the gain-of-function mutation in the ERK2 regulation network is the result of coupling of several enzymatic processes that work in opposite directions.

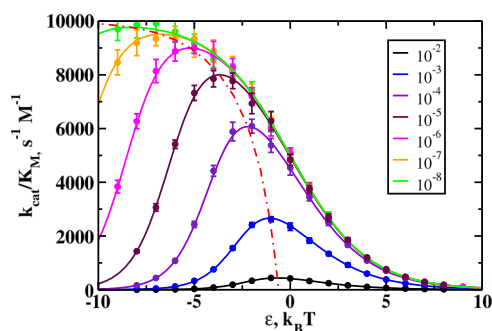


**FIG. 5.** The specificity constant as the function of the interaction energy for varying concentrations of deactivator. Lines are theoretical predictions, and symbols correspond to kinetic Monte Carlo simulations. Error bars show standard deviations. Numbers in the legend show the concentrations of the deactivator  $D$  in units of moles per liter. Dashed line shows the position of the maximum of the specificity constant.

Theoretical calculations presented in Fig. 5 also lead to a surprising prediction that the sign of the mutation effect (positive gain-of-function, or negative loss-of-function) can be reversed by changing the concentration of one of the network components, namely, the deactivators. For example, if one assumes that the sevenmaker mutation operates in the range of interaction strengths as given in Fig. 4 (between two vertical lines), then for very low concentrations of the deactivator molecules (less than  $10^{-5}$  M), this mutation (increasing  $\epsilon$  from  $-4$  to  $-1$   $k_B T$ ) will no longer be increasing the enzymatic activity. We speculate that this ability of the network to selectively affect the efficiency of enzymatic processes might be an additional level of regulation that can benefit cellular functioning.

Our theoretical views can be further supported by analyzing the turnover times as a function of the interaction energies, as illustrated in Fig. 6. One can see that the effective overall catalytic rate (inverse turnover times) shows the nonmonotonic behavior for both the simple MM and the ERK2 regulation pathways. But there is a range of interaction energies where the increase in the binding energy lowers the rate of the MM process, while the process in the ERK2 regulation network can go faster. This is an additional argument to explain the existence of the gain-of-function mutations and specifically the effect of the sevenmaker mutation in ERK2. Even if the mutation lowers the rate along each enzymatic pathway (considered separately), it might effectively increase the overall rate in the complex ERK2 scheme that combines all of them.

It is also worth mentioning that all our theoretical and simulation results correspond to the stationary state conditions. Figures S1–S4 show the results of additional computer simulations starting from the phosphorylated ERK2. As seen from Fig. S4, the predicted turnover time does not depend on the starting state (ERK2 or ppERK2), as expected for the steady-state situations.

Because our theoretical approach makes semiquantitative predictions, it is important to compare them with experimental observations. However, experimental data on sevenmaker mutations are

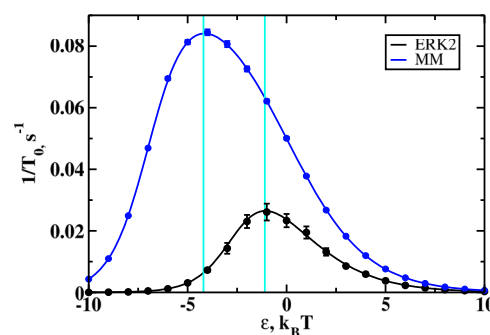


**FIG. 6.** Inverse catalytic turnover times, or the effective overall reaction rates for the product formation, as a function of the interaction energy for the Michaelis-Menten scheme (MM, blue) and for the ERK2 scheme (black). Lines are theoretical predictions, and symbols correspond to kinetic Monte Carlo simulations. Error bars show standard deviations. Concentration of the substrate is  $S = 10^{-5}$  M. In the region between two vertical lines, decrease of interaction energies leads to decrease of the reaction rate for the simple MM scheme, but for the ERK2 network, it leads to the increased turnover rate.

pretty scarce, mostly qualitative, and obtained using very different techniques and under different experimental conditions. This prevents us from explicitly including them into our analysis. But we notice that Camps *et al.*<sup>40</sup> found that about one order of magnitude higher concentrations of MKP-3 are needed in order to deactivate the mutated  $ERK2^{D319N}$  protein variant as compared with the wild type  $ERK2$ . In addition, the decrease of deactivation activity by other phosphatases (PAC1, MKP-1, and MKP-2, approximately from 3 to 7 times lower) for mutated  $ERK2$  species was reported by Chu *et al.*<sup>37</sup> All these observations are consistent with our theoretical flux arguments. We suggest that the sevenmaker mutation lowers the flux through the deactivation branch and this makes the flux to reach the final product larger, leading to the overall increase in the enzymatic activity of mutated  $ERK2$  species. Furthermore, experimental data by Tanoue *et al.*<sup>35</sup> show that the activation of  $ERK2$  by MEK1 is less sensitive to the sevenmaker mutation: MEK1-facilitated activation activity of mutated  $ERK2$  is only 0.88 of that for WT  $ERK2$ . However, phosphorylation activity of  $ERK2$  toward substrate MNK1 is strongly affected by the mutation: phosphorylation activity of mutant  $ERK2$  is estimated of being 0.11 of that of the WT enzyme. This suggests that all the processes involving  $ERK2$  can be negatively affected by the sevenmaker mutation to a different degree. It also means that the overall balance of these effects *in vivo* is difficult to explicitly estimate since there are many known activators, deactivators, and substrates of  $ERK2$ ,<sup>35</sup> and likely many more will be discovered in the future.

#### IV. CONCLUSIONS

We developed a kinetic network model to explain the observations of the increased enzymatic activity in the enzymes with the sevenmaker mutation and for other similar gain-of-function mutations in the  $ERK2$  enzymes. Our approach presents a comprehensive “semiquantitative” description of the enzymatic properties of the wild-type and mutated  $ERK2$  regulation systems. First, we constructed a simplified regulation network for  $ERK2$  by arguing that it can be viewed as three coupled Michaelis-Menten processes that describe three main enzymatic processes: activation, deactivation, and phosphorylation. The corresponding kinetic scheme is then analyzed explicitly using the method of first-passage processes to evaluate the enzymatic properties of the system in terms of the individual transition rates and the binding energy between the enzyme and the substrates. The obtained analytical results are also compared with the predictions for the simple Michaelis-Menten scheme.

It is argued that mutations modify the interaction energies, and this leads to changes in the enzymatic features of the mutant  $ERK2$  molecules. Our calculations show that the catalytic properties of  $ERK2$  differ significantly from the results for the simplest Michaelis-Menten process. We found a nonmonotonic dependence of the specificity constant, which is a quantitative measure of the enzymatic efficiency, as a function of the interaction energy. This suggests that some mutations might increase the activity of the enzyme by changing the interaction energies to the values closer to the observed maximum. The proposed mechanism is also discussed in terms of the fluxes via different branches of the regulation network, and theoretical calculations generally support it. Thus, our main conclusion is that the sevenmaker mutation modifies the

binding interaction energy in such way that the deactivation process is affected less than the activation processes, leading to the effective increase in the overall catalytic activity. While the mutation lowers the rate for each enzymatic branch for some interactions' energies, the overall turnover time might at the same time decrease, making them catalytically more active. These theoretical predictions agree with known experimental observations. In addition, it was suggested that the effect of mutation (positive or negative) might be affected by the concentration of activator, deactivator, and substrate molecules that participate in the  $ERK2$  regulation network.

Our theoretical model provides a consistent chemical description of the possible mechanisms for the gain-of-function mutations in  $ERK2$ , giving a fully quantitative measure of mutations, which can be in principle experimentally measured. However, it is important to discuss the limitations of the proposed theoretical method. A weak side of our approach is that a very complex biochemical network with multiple states and transitions, which controls the activities of  $ERK2$  enzymes, is simplified into a network with only three coupled Michaelis-Menten processes. It is also assumed that the reaction constants for activation, deactivation, and phosphorylation are the same while they might differ significantly. In addition, current experiments give only very qualitative measurements of the increase of enzymatic activities of the mutant  $ERK2$  molecules. But our hope is that the presented semiquantitative model will stimulate experimental and theoretical studies that will test our ideas, thus advancing our understanding on the mechanisms of functioning of the  $ERK2$  as well as other regulating enzymatic systems.

#### SUPPLEMENTARY MATERIAL

See [supplementary material](#) for results of additional Monte Carlo simulations with relaxed parameters of the model as well as simulations starting from phosphorylated state of  $ERK2$  to show that results presented here correspond to the stationary state.

#### ACKNOWLEDGMENTS

This work was supported by the Center for Theoretical Biological Physics NSF Grant No. PHY-1427654. A.B.K. also acknowledges the support from the Welch Foundation (Grant No. C-1559) and the NSF (Grant No. CHE-1664218).

#### APPENDIX A: DERIVATION OF BACKWARD MASTER EQUATIONS

Backward Master Equations (BMEs) are closely related to ordinary chemical kinetic equations and are derived in a similar manner. We define  $F_{i,N}(t)$  as a probability for the random walker to reach the state  $N$  for the first time if at  $t = 0$  it started from the state  $i$ . To understand how BMEs are obtained, we consider all first-passage trajectories that start from the state  $i$  and finish in the state  $N$ . If from the state  $i$ , the system can go to the states  $i - 1$  and  $i + 1$ , then all trajectories can be divided into 2 groups. The corresponding first-passage probability  $F_{i,N}(t)$  is related to two first-passage probabilities,  $F_{i-1,N}(t)$  and  $F_{i+1,N}(t)$ . BME for the state  $i$  reflects this



relation by considering the temporal evolution of these probabilities. In addition, the final state in our system is always State 5, so we omit  $N$  and write just  $F_i(t)$  to simplify the notations.

To illustrate, let us take as an example State 0 (Fig. 1 in the main paper); then, there is only one reaction leading from this state with the rate constant  $u$  to State 1. So the BME for this state is written as

$$\frac{dF_0(t)}{dt} = u_M F_1(t) - u_M F_0(t). \quad (\text{A1})$$

From the State 1, there are two outgoing reactions with rate constants  $w$  and  $\alpha$  leading to states 0 and 2, respectively, and so the BME for this state is given by

$$\frac{dF_1(t)}{dt} = \alpha F_2(t) + w F_0(t) - (w + \alpha) F_1(t). \quad (\text{A2})$$

Similar arguments are applied for derivation of BME for all other states.

## REFERENCES

- 1 A. S. Futran, A. J. Link, R. Seger, and S. Y. Shvartsman, *Curr. Biol.* **23**, R972 (2013).
- 2 H. Lavoie and M. Therrien, *Nat. Rev. Mol. Cell Biol.* **16**, 281 (2015).
- 3 J. A. McCubrey, L. S. Steelman, W. H. Chappell, S. L. Abrams, G. Montalto, M. Cervello, F. Nicoletti, P. Fagone, G. Malaponte, M. C. Mazzarino, S. Candido, M. Libra, J. Bäsecke, S. Mijatovic, D. Maksimovic-Ivanic, M. Milella, A. Tafuri, L. Cocco, C. Evangelisti, F. Chiarini, and A. M. Martelli, *Oncotarget* **3**, 954 (2012).
- 4 M. H. Cobb and E. J. Goldsmith, *J. Biol. Chem.* **270**, 14843 (1995).
- 5 Y. Kim, Z. Paroush, K. Nairz, E. Hafen, G. Jiménez, and S. Y. Shvartsman, *Mol. Syst. Biol.* **7**, 467 (2011).
- 6 F. Zhang, A. Strand, D. Robbins, M. H. Cobb, and E. J. Goldsmith, *Nature* **367**, 704 (1994).
- 7 B. J. Canagarajah, A. Khokhlatchev, M. H. Cobb, and E. J. Goldsmith, *Cell* **90**, 859 (1997).
- 8 J. Zhang, P. Shapiro, and E. Pozharski, *Acta Crystallogr., Sect. F: Struct. Biol. Cryst. Commun.* **68**, 1434 (2012).
- 9 J. J. Seidel and B. J. Graves, *Genes Dev.* **16**, 127 (2001).
- 10 Á. Garai, A. Zeke, G. Gógl, I. Törő, F. Fördős, H. Blankenburg, T. Bárkai, J. Varga, A. Alexa, D. Emig, M. Albrecht, and A. Reményi, *Sci. Signaling* **5**, ra74 (2012).
- 11 D. L. Sheridan, Y. Kong, S. A. Parker, K. N. Dalby, and B. E. Turck, *J. Biol. Chem.* **283**, 19511 (2008).
- 12 D. Jacobs, D. Glossip, H. Xing, A. J. Muslin, and K. Kornfeld, *Genes Dev.* **13**, 163 (1999).
- 13 S. Lee, M. Warthaka, C. Yan, T. S. Kaoud, P. Ren, and K. N. Dalby, *Biochemistry* **50**, 9500 (2011).
- 14 O. Abramczyk, M. A. Rainey, R. Barnes, L. Martin, and K. N. Dalby, *Biochemistry* **46**, 9174 (2007).
- 15 C. M. Slupsky, L. N. Gentile, L. W. Donaldson, C. D. Mackereth, J. J. Seidel, B. J. Graves, and L. P. McIntosh, *Proc. Natl. Acad. Sci. U. S. A.* **95**, 12129 (1998).
- 16 A. D. Sharrocks, S.-H. Yang, and A. Galanis, *Trends Biochem. Sci.* **25**, 448 (2000).
- 17 S. M. Carlson, C. R. Chouinard, A. Labadorf, C. J. Lam, K. Schmelzle, E. Fraenkel, and F. M. White, *Sci. Signaling* **4**, rs11 (2011).
- 18 S. Yoon and R. Seger, *Growth Factors* **24**, 21 (2006).
- 19 B. Zhou, L. Wu, K. Shen, J. Zhang, D. S. Lawrence, and Z.-Y. Zhang, *J. Biol. Chem.* **276**, 6506 (2001).
- 20 N. G. Anderson, J. L. Maller, N. K. Tonks, and T. W. Sturgill, *Nature* **343**, 651 (1990).
- 21 T. Lee, A. N. Hoofnagle, K. A. Resing, and N. G. Ahn, *J. Mol. Biol.* **353**, 600 (2005).
- 22 K. M. Sours, S. C. Kwok, T. Rachidi, T. Lee, A. Ring, A. N. Hoofnagle, K. A. Resing, and N. G. Ahn, *J. Mol. Biol.* **379**, 1075 (2008).
- 23 J. Zhang, F. Zhang, D. Ebert, M. H. Cobb, and E. J. Goldsmith, *Structure* **3**, 299 (1995).
- 24 K. M. Sours, Y. Xiao, and N. G. Ahn, *J. Mol. Biol.* **426**, 1925 (2014).
- 25 Y. Xiao, T. Lee, M. P. Latham, L. R. Warner, A. Tanimoto, A. Pardi, and N. G. Ahn, *Proc. Natl. Acad. Sci. U. S. A.* **111**, 2506 (2014).
- 26 M. J. Robinson, M. Cheng, A. Khokhlatchev, D. Ebert, N. Ahn, K.-L. Guan, B. Stein, E. Goldsmith, and M. H. Cobb, *J. Biol. Chem.* **271**, 29734 (1996).
- 27 S. J. Mansour, W. T. Matten, A. S. Hermann, J. M. Candia, S. Rong, K. Fukasawa, G. V. Woude, and N. G. Ahn, *Science* **265**, 966 (1994).
- 28 L. Colucci-D'Amato, C. Perrone-Capano, and U. di Porzio, *BioEssays* **25**, 1085 (2003).
- 29 M. C. Lawrence, A. Jivan, C. Shao, L. Duan, D. Goad, E. Zaganjor, J. Osborne, K. McGlynn, S. Stippec, S. Earnest, W. Chen, and M. H. Cobb, *Cell Res.* **18**, 436 (2008).
- 30 A. Plotnikov, E. Zehorai, S. Procaccia, and R. Seger, *Biochim. Biophys. Acta, Mol. Cell Res.* **1813**, 1619 (2011).
- 31 D. Brunner, N. Oellers, J. Szabad, W. H. Biggs III, S. L. Zipursky, and E. Hafen, *Cell* **76**, 875 (1994).
- 32 C. M. Bott, S. G. Thorncroft, and C. J. Marshall, *FEBS Lett.* **352**, 201 (1994).
- 33 N. Oellers and E. Hafen, *J. Biol. Chem.* **271**, 24939 (1996).
- 34 F. D. Karim and G. M. Rubin, *Mol. Cell* **3**, 741 (1999).
- 35 T. Tanoue, M. Adachi, T. Moriguchi, and E. Nishida, *Nat. Cell Biol.* **2**, 110 (2000).
- 36 J. Zhang, B. Zhou, C.-F. Zheng, and Z.-Y. Zhang, *J. Biol. Chem.* **278**, 29901 (2003).
- 37 Y. Chu, P. A. Solski, R. Khosravi-Far, C. J. Der, and K. Kelly, *J. Biol. Chem.* **271**, 6497 (1996).
- 38 N. G. Van Kampen, *Stochastic Processes in Physics and Chemistry*, 3rd ed. (North Holland, 2007).
- 39 A. B. Kolomeisky, *Motor Proteins and Molecular Motors* (CRC Press, 2015).
- 40 M. Camps, A. Nichols, C. Gillieron, B. Antonsson, M. Muda, C. Chabert, U. Boschert, and S. Arkininstall, *Science* **280**, 1262 (1998).